Development of Seismic Fragility Functions for a Moment Resisting Reinforced Concrete Framed Structure

D. P. McCrum, G. Amato[*] and R. Suhail

School of Planning, Architecture and Civil Engineering, Queen's University of Belfast, Belfast, United Kingdom

Abstract: Understanding the seismic vulnerability of building structures is important for seismic engineers, building owners, risk insurers and governments. Seismic vulnerability defines a buildings predisposition to be damaged as a result of an earthquake of a given severity. There are two components to seismic risk; the seismic hazard and the exposure of the structural inventory to any given earthquake event. This paper demonstrates the development of fragility curves at different damage states using a detailed mechanical model of a moment resisting reinforced concrete structure typical of Southern Europe. The mechanical model consists of a complex three-dimensional finite element model of the reinforced concrete moment resisting frame structure and is used to define the damage states through pushover analysis. Fragility curves are also defined using the HAZUS macro-seismic methodology and the Risk-UE macro-seismic methodology. Comparison of the mechanically modelled and HAZUS fragility curve shows good agreement while the Risk-UE methodology shows reasonably poor agreement.

1. INTRODUCTION

Seismic risk of the built environment comprises of the earthquake hazard and the exposure of the built environment to earthquake damage. The seismic hazard is defined through seismic hazard maps [1] which represent the likelihood of a certain ground motion on a local, regional and national level. The level of potential ground motion on a site depends on the type of faults *e.g.* dip-slip or strike-slip, in the area under consideration and on their size.

Within seismic hazard analysis the mapping of European countries through the SHARE project [2] has resulted in greatly improved seismic hazard maps that are open source. Moreover, collaborative projects involving data collection and web-based computational platforms such as the Global Earthquake Model (GEM) Project (www.globalquakemodel.org) and OpenQuake [3] are pushing the development of risk assessment at global, national and local scales.

To assess the exposure of a built area to seismic damage a macro-seismic vulnerability method has been classically used [4]. This approach, based on observed and statistically analysed damage, classifies the existing building stocks in terms of structural typology, material and design code level. One of the issues of concern within the field of seismic risk assessment is the lack of detail used to characterise the existing building stock. Often, the height (therefore the period of vibration), construction type *e.g.* steel/reinforced concrete and date of construction *i.e.* whether seismic design codes were used or not, are the only parameters taken into consideration. This is understandable, particularly coming from a city planning or catastrophe risk insurance point of view where detailed classification of building stock is limited. This project aims to provide some physically modelled seismic structural response data to aid validation of the fragility curves achieved through statistical methodologies.

The exposure is calculated by computing fragility functions, that is by measuring the probability of each building type of exceeding a quantified set of damage states.

* Address correspondence to this author at the School of Planning, Architecture and Civil Engineering, David Keir Building, Queen's University Belfast, BT9 5AG, United Kingdom; Tel: +44 (0)28 9097 4006; Fax: +44 (0)28 9097 4278; E-mail: g.amato@qub.ac.uk

These damage states are typically levels of displacement drift in a structure in which for example the structure first yields, reaches ultimate limit state or collapses. Finally, the seismic risk is represented by a vulnerability function which is the probabilistic distribution of a loss ratio conditional on a certain level of ground motion [5] and depends on both the structural stock exposure and the local seismic hazard.

In this paper, the vulnerability curves of a medium height framed reinforced concrete (RC) structure obtained using macro-seismic approaches are assessed using a sophisticated Finite Element (FE) model of a three-storey moment resisting RC sub-frame. A pushover analysis is performed on the structure and damage states are defined by visual observation and a mechanical method presented in the framework of the Risk-UE project [6, 7], a European project aiming at assessing earthquake scenarios on European cities with regard to current and historical buildings. The damage states are then compared to those defined through the HAZUS [8] macro-seismic method.

The structure has been designed according to Eurocode 8 [9] and Eurocode 2 [10] and is typical of modern construction within Europe. Many seismic risk studies have been performed on existing non-code designed RC structures to better understand their performance, however few exist on more recently constructed buildings.

2. PUSHOVER ANALYSIS OF A THREE-DIMENSIONAL REINFORCED CONCRETE FRAMED STRUCTURE

A pushover analysis of the moment resisting frame structure shown in Fig. (**1**) has been carried out to obtain the base shear force *vs.* lateral roof displacement capacity curve. The structure has been designed using the EC8 pushover method which is an equivalent static method of analysis for multi-degree-of-freedom (MDOF) structures in which the inertia forces are estimated and applied as a horizontal load pattern. In a pushover analysis, the static horizontal forces are applied to the locations of lumped masses, in this case to the floor diaphragms. The load pattern is then incrementally applied to the structure typically using a finite element program to obtain a curve of base shear force *vs.* displacement of a control point, usually located on the roof. The following design parameters have been used to calculate the lateral pushover forces; soil type B, peak ground acceleration, $a_g = 0.16g$ and a behaviour factor, $q = 4$.
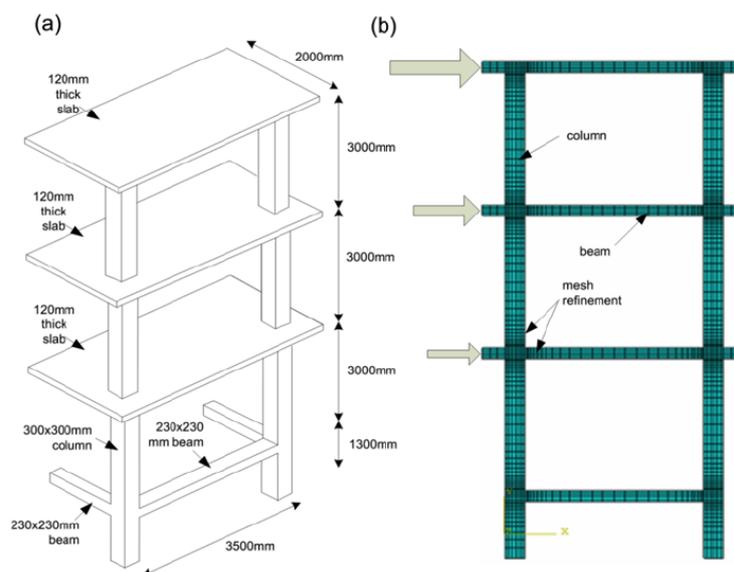
Fig. (1). Three-dimensional (**a**) schematic; and (**b**) finite element model of the moment resisting reinforced concrete framed substructure analysed.

It is important to note that the parameters of lateral displacement and base shear force calculated during the pushover analysis do not allow direct comparison with spectral demand [4]. Using the modal properties and the equivalent single-degree-of-freedom system (SDOF) approach the base shear force is converted to spectral acceleration and lateral roof displacement is converted to spectral displacement [4]. This results in a capacity curve that is defined in terms of the spectral quantities allowing the fragility curve to be generated.

The portion of the structure computationally modelled is a three-storey single bay moment resisting RC frame with a plinth beam at 1.3m from the foundation as shown in Fig. (**1a**). Only one sub-frame of a typical three-storey building

was computationally modelled to reduce computational time and demand. The pushover load pattern has been calculated for the sub-frame of the building shown in Fig. (**1a**). Therefore, the results are scalable to an entire framed structure. Each storey height in the building is 3.0m, with column cross-sections of 300 mm x 300 mm and beam cross-sections of 230 mm x 230 mm throughout. Floor slabs are 120 mm in thickness. Concrete cover in columns and beams was taken as 30 mm and 25mm, respectively. All floors were loaded with a uniformly distributed superimposed dead load of 1kN/m^2 and live load of 2.5kN/m^2. A compressive strength of 34 N/mm^2 is used for the concrete in thisstudy. The material properties of the reinforcing steel are given in Table **1**.

Table 1. Material properties for steel reinforcement.

Bar Dia. (mm)	Steel Use	E_o (GPa)	f_y (MPa)	f_u (MPa)
8	Column Shear Link Bar	214	551	643
10	Beam Shear Link Bar	213	447	538
16	Column Longitudinal Bar	214	420	541
20	Beam Longitudinal Bar	210	449	568

A finite element model of the building was developed in ABAQUS 6.13 [11] as shown in Fig. (**1b**). In this study Concrete Damage Plasticity Model (CDPM) developed by Lubliner *et al.* [12] with modifications proposed by Lee and Fenves [17] is used. CDPM in ABAQUS uses the concept of isotropic damage and is used in combination with the isotropic tensile and compressive plasticity to represent the nonlinear behaviour of the concrete [13]. CDPM in ABAQUS is defined using uniaxial compression and tension response of concrete, and requires five constitutive parameters to define the shape of yield surface and flow potential surface [11].

In this study the constitutive law for uniaxial compression response of the unconfined concrete proposed by Thorenfeldt [14]. Tension response of the concrete is defined using the stress-crack opening displacement relationship proposed by Hordijk [15]. Fracture energy required to define tension softening of concrete is calculated using the expression

$G_f = 73 \, fc^{0.18}$ given in CEB-FIB Model Code 2010 [16]. The constitutive parameters used to define yield surface and flow potential surface are: dilation angle(ψ),flow potential eccentricity(ε), ratio of strength of concrete under biaxial compression to the strength under uniaxial compression (f_{b0}/f_{c0}), ratio of strength of concrete under biaxial compression to strength under tri-axial compression (K) and viscosity parameter (μ). Values of these constitutive parameters used in this study are shown in Table **2** and are based on literature research on CDPM [17 - 19].

The RC frame is modelled using 3D brick elements and 2D truss elements. The 8 node C3D8R linear brick element is used to model the nonlinear behaviour of the concrete frame. C3D8R is a first order continuum stress/displacement solid finite element capable of satisfactorily capturing the nonlinear response of concrete when used with hourglass stiffness control. The enhanced hourglass stiffness option available in ABAQUS is used to alleviate the effect of zero energy modes due to reduced integration. The steel reinforcement is modelled using a 2 node 2D truss element, namely T3D2. Reinforcement is embedded inside the concrete frame using embedded technique which assumes a perfect bond between reinforcement and concrete. A mesh sensitivity analysis was performed to ensure solution accuracy at critical locations such as the beam-column, whilst minimisingmesh refinement at less critical locations in order to reduce the computation time.

3. CAPACITY CURVE RESULTS

The base shear force *vs.* lateral roof displacement curve obtained from the lateral pushover analysis of the sub-frame performed according to EC8 is shown in Fig. (**2**). The model failed due to lack of convergence at 238.33 mm. This does

Table 2. ABAQUS concrete damage plasticity model parameters.

Ψ (deg)	ε	$\dfrac{f_{b0}}{f_{co}}$	K	M
36°	0.1	1.16	2/3	10^{-7}
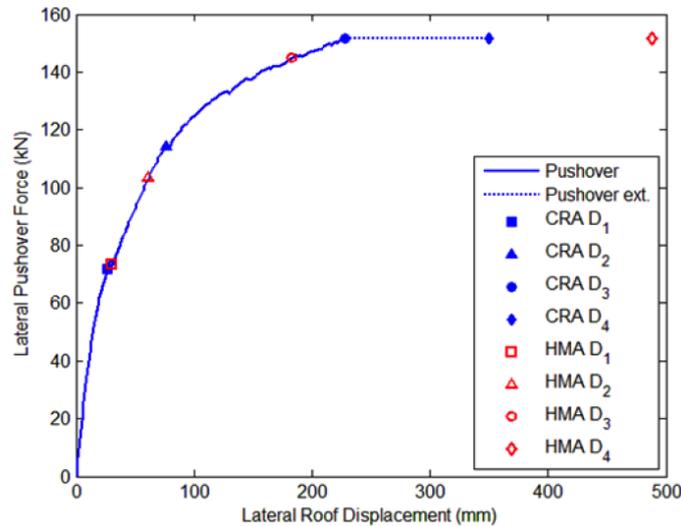
Fig. (2). Pushover curve for reinforced concrete moment resisting framed substructure.

not equate to actual collapse of the structure, just numerical failure of the computer model. Based on engineering judgement and assessment of the stress distribution in the structure at the final time step, collapse was estimated to occur at a lateral roof displacement of approximately 350 mm. This can be seen in Fig. (**2**) as the 'Pushover ext.' portion of the curve.

3.1. Damage States

Damage states are used in HAZUS to evaluate casualties and monetary losses due to building damage and closure after natural hazard events. Median values and standard deviation of spectral displacement corresponding to *slight*, *moderate*, *extensive* and *complete* damage states are given for building typology, average height and design code level.

The damage states, comprising of a damage-based description of the state of the three-storey reinforced concrete moment resisting framed structure (LC1 classification) designed according to high level code (EC8) as defined in HAZUS are reported in Table **3**. The HAZUS methodology is referred to as the HAZUS Macro-seismic Approach (HMA) herein. In Table **3** the median values are compared to those obtained by inspection of the FE model subjected to pushover (referred to as the Capacity Response Approach (CRA)) and identified using the damage state descriptions. From Fig. (**2**) it can be seen that the D_1 limit of 26.66 mm lateral roof displacement is obtained after the yield capacity is reached. This lateral roof displacement represents the initiation of damage in the structure.

The D_2 limit can be seen in Fig. (**2**) as the end of slight structural damage at a lateral roof displacement of 76.66mm. The capacity curve shows the stiffness of the structure reducing noticeably. Fig. (**3**) presents the CRA finite element model results at the limit of damage state D_2. Most beams and columns can be seen to have stress concentrations above yield and hairline cracks would be observed in multiple locations.

The limit of extensive structural damage D_3 is defined as the end of the numerical analysis. The analysis failed after a roof displacement of 228.33 mm as can be seen in Table **3** and Fig. (**2**). Fig. (**4**) presents the finite element model results at the limit of damage state D_3. The concrete would have spalled with large flexural cracks being observed. The beams have all yielded with plastic hinges formed at beam end locations as shown in Fig. (**4**). The lateral stiffness of the structure can be seen to be very small in Fig. (**2**). Column members have high stress concentrations indicating significant cracking at roof and ground floor as can be seen in Fig. (**4**). The structure still has some lateral stiffness and is estimated to collapse (D_4) at approximately 350 mm; however as mentioned previously this lateral roof displacement was not reached during analysis.
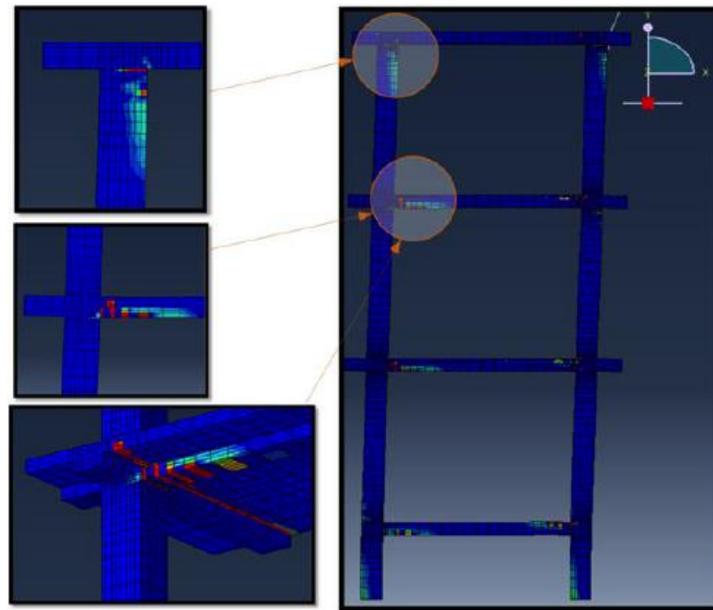
Fig. (3). Screenshot view of finite element analysis of moment resisting reinforced concrete framed structure at D_2 limit.

In Fig. (**2**) the yielding and ultimate capacity from the HMA and damage limits identified directly from the pushover curve are plotted. On the pushover curve the yielding point has been chosen as the final point of the linear behaviour (8.32 mm) and the ultimate capacity at the formation of the plastic mechanism and corresponding failing of the finite element simulation.

To convert the capacity curve of the SDOF system to spectral quantities associated to the MDOF structure the HAZUS approach is used. The yielding spectral acceleration is calculated as a function of the design strength coefficient , the fraction of building weight effective in pushover mode, and overstrength factor, which relates the real yield strength to the design value where;

$$A_y = C_s \gamma / \alpha_1 \tag{1}$$

Table 3. Damage state definitions and spectral displacement for HAZUS Macro-seismic Approach (HMA) and Capacity Response Approach (CRA) displacements.

| Damage State	Description(Hazus)	HMA Roof Disp. (mm)	CRA Roof Disp. (mm)	Difference (%)
D_1	**Slight Structural Damage:** Flexural or shear type hairline cracks in some beams and columns near joints or within joints.	30.48	26.66	14.3
D_2	**Moderate Structural Damage:** Most beams and columns exhibit hairline cracks. In ductile frames some of the frame elements have reached yield capacity indicated by larger flexural cracks and some concrete spalling. Non ductile frames may exhibit larger shear cracks and spalling.	60.96	76.66	-20.5
D_3	**Extensive Structural Damage:** Some of the frame elements have reached their ultimate capacity indicated in ductile frames by large flexural cracks, spalled concrete and buckled main reinforcement; non ductile frame elements may have suffered shear failures or bond failures at reinforcement splices, or broken ties or buckled main reinforcement in columns which may result in partial collapse.	182.88	228.33	-19.9
D_4	**Complete Structural Damage:** Structure is collapsed or in imminent danger of collapse due to brittle failure of non ductile frame elements or loss of frame stability.	487.68	350	39.3
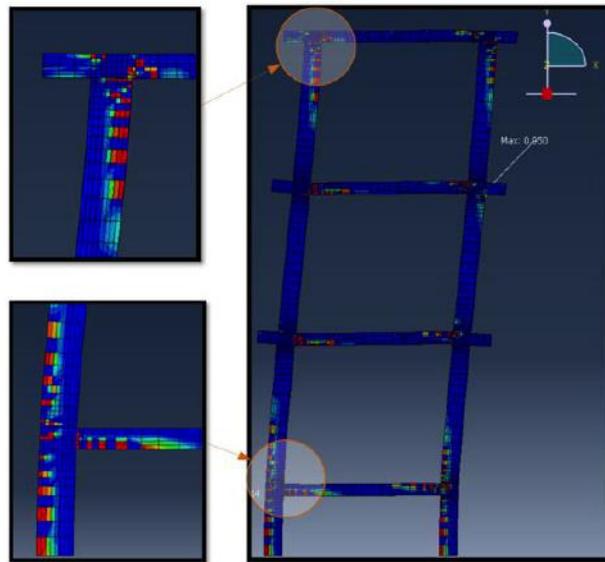
Fig. (4). Screenshot view of finite element analysis of moment resisting reinforced concrete framed structure at D_3 limit.

The yielding spectral displacement, $S_{d,y}$ is obtained as a function of the elastic period of the structure, T_e ;

$$S_{d,y} = 9.81 A_y T_e^2 \tag{2}$$

Ultimate spectral values are given as a function of ductility, μ and overstrength ratio, λ where;

$$A_u = \lambda A_y \tag{3}$$

$$S_{d,u} = \lambda \mu D_y \tag{4}$$

All coefficients are reported in tables according to the structure type and level of design code in HAZUS. Spectral displacement, $S_{d,k}$ and acceleration, $A_{d,k}$ are related to lateral roof displacement, D_k and base shear force, F respectively, by the height response factors, α_2 and the fraction of building weight, W at location of pushover mode displacement, α_1 as follows;

$$S_{d,k} = \alpha_2 \, D_k \tag{5}$$

$$A_{d,k} = \alpha_1 \, W \, F \tag{6}$$

4. ALTERNATIVE MECHANICAL APPROACH

In order to use an automatic procedure for defining the idealisedelasto-plastic capacity curve corresponding to a pushover force-displacement curve, EC8 defines the yielding displacement, D_y as the displacement for which the energy associated to the two curves is the same, see Fig. (**5**). This value does not represent the end of the elastic curve of the structure nor the real yield capacity. According to this approach in the RISK-UE project [7], referred to as the Risk-UE Mechanical Approach (RMA) herein, the damage state limits are set as a function of the yielding, D_y and ultimate displacements D_u;

$$D_1 = 0.7 D_y \tag{7}$$

$$D_2 = 1.5 D_y \tag{8}$$

$$D_3 = 0.5(D_y + D_u) \tag{9}$$

$$D_4 = D_u \tag{10}$$

The RMA damage limit states were defined to be representative of the EMS-98 [20] macro-seismic scale. A description of the structural damage corresponding to each limit state is given in Table **4**. By applying the procedure to the frame used in this paper the values reported in Table **4** are obtained and compared with the CRA values.
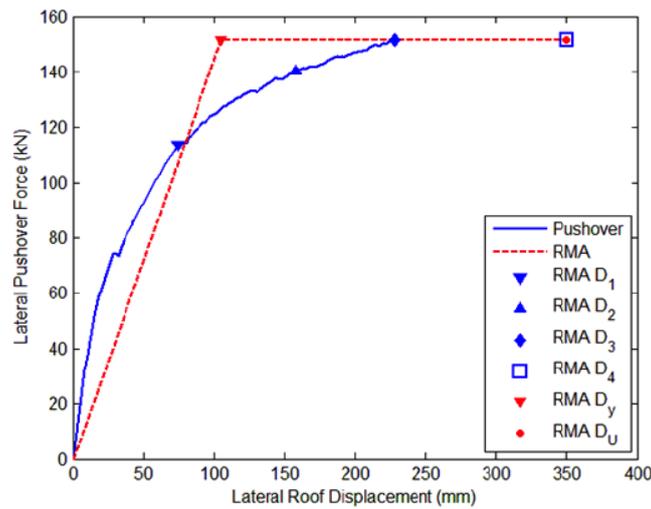

Fig. (5). Pushover curve (CRA) with RMA damage states and idealised elastoplastic curve.

5. FRAGILITY CURVES

The fragility curves are defined according to Eq. (11) as defined in HAZUS. The probability of being in or exceeding a given damage state is modelled as a cumulative lognormal distribution. Given the spectral displacement, *Sd*, the probability of structural damage being in or exceeding a damage state, d_s, is modelled as:

Table 4. EMS-98 damage limit states and displacements of the test structure.

Damage State	Description (EMS-98)	RMA Roof Disp. (mm)	CRA Roof Disp. (mm)	Difference (%)
D_1	Weak/No Structural damage For columns and beams, the deformation does not exceed elastic limit. Only inter-storey drift-sensitive non-structural components are considered.	74	26.66	73.6
D_1	Moderate/Low Structural damage For columns and beams considered as primary components the deformation not exceed 25% of the ultimate value.	158	76.66	106.1
D_1	Significant/Medium Structural damage For columns and beams considered as primary components the deformation not exceed three quarters (75%) of the ultimate value.	228	228.33	0.1
D_1	Heavy Structural damage/Collapse For columns and beams considered as primary components deformation exceeds three quarters (75%) of the ultimate value and at most one structural element exceed the ultimate value.	350	350	0.0

$$P[d_s|s_d] = \Phi\left[\frac{1}{\beta_{ds}}\ln\left(\frac{s_d}{\bar{s}_{d,ds}}\right)\right] \tag{11}$$

where; $\bar{S}_{d,ds}$ is the median value of spectral displacement at which the building reaches the threshold of the damage state, d_s; β_{ds} is the standard deviation of the natural logarithm of spectral displacement of damage state, d_s and Φ is the standard normal cumulative distribution function.

In HAZUS the lognormal standard deviation of the fragility curves is defined as a function of the standard deviation of the capacity curve, the variability of the demand spectrum and the uncertainty in the estimate of the median value of

the structural damage spectral displacement. In the RMA the standard deviation was estimated as a function of the structure ductility as $\beta=0.4 \ln(\mu)$.

The values of median and standard deviation are reported in Table **5** together with the damage limit spectral displacements obtained from the pushover curve (CRA). In Fig. (**6**) the corresponding fragility curves are plotted and the median values are compared with the spectral displacement limit from the pushover curve. The probabilities associated to the spectral displacements are reported in Table **6**.

Table 5. Structural fragility curves: medians and standard deviations.

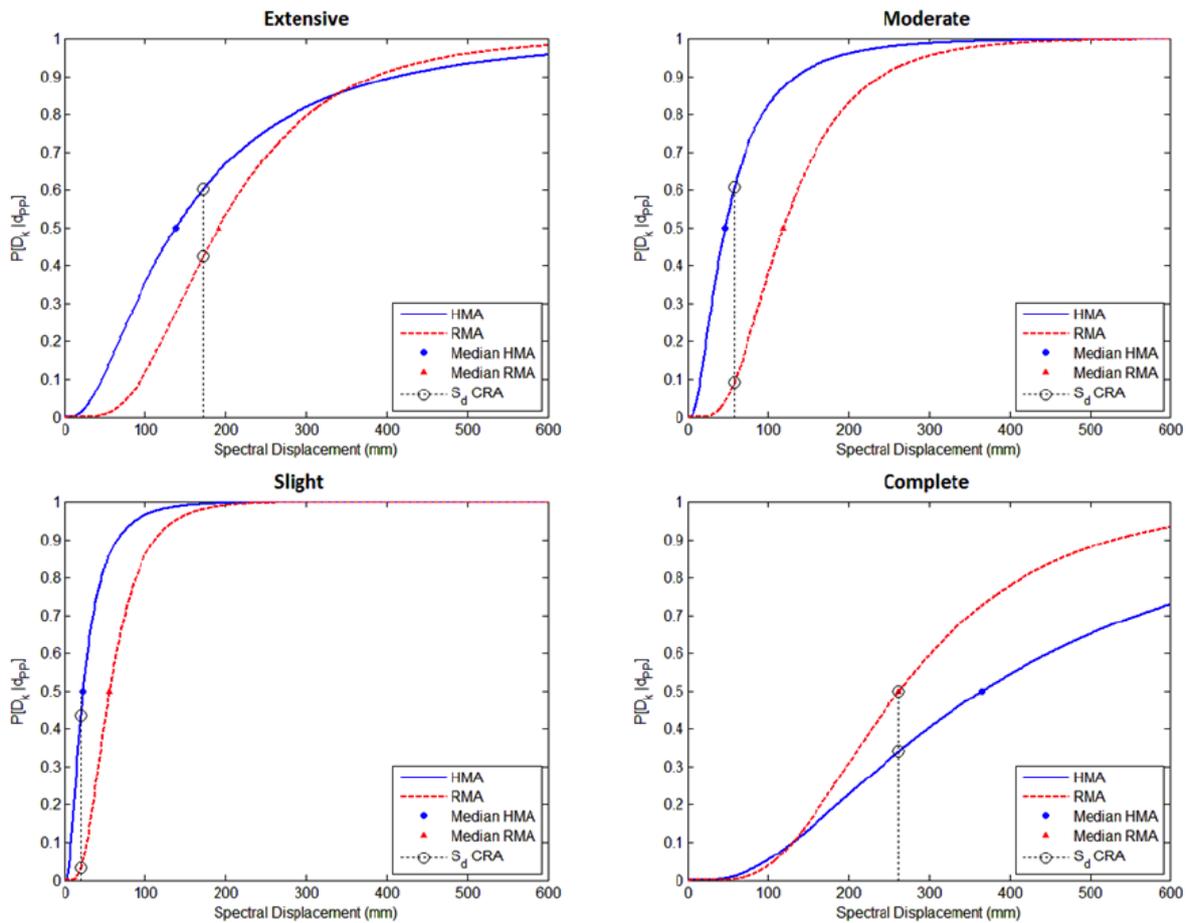|	CRA Capacity Response Approach	HMA HAZUS Macro-seismic Approach		RMA Risk-UE Macro-seismic Mechanical Approach	
	S_d (mm)	Median (mm)	Beta	Median (mm)	Beta
Slight	20.0	22.9	0.81	55.2	0.55
Moderate	57.5	45.7	0.84	118.3	0.55
Extensive	171.2	137.2	0.86	190.4	0.55
Complete	262.5	365.8	0.81	262.5	0.55

Fig. (6). Fragility curves for slight, moderate, extensive and complete damage states obtained using the RMA & HMA methods.

As expected the two sets of curves yield to quite different results, especially for the *slight* and *moderate* median values. Median values for these two limit states are based on the yielding displacement value calculated as the displacement for which the idealisedelasto-plastic curve has the same energy of the original push over curve. This means that the more the capacity curve shows a plastic trend, the higher is the yielding displacement.

Table 6. HMA and RMA fragility curve values associated to the spectral displacements of the numerical model (CRA).

	CRA Capacity Response Approach	HMA HAZUS Macro-seismic Approach	RMA Risk-UE Macro-seismic Mechanical Approach
	S_d (mm)	$P[D_k|dpp]$ (%)	$P[D_k|dpp]$ (%)
Slight	20.0	45.5	3.3
Moderate	57.5	60.8	9.5
Extensive	171.2	60.2	42.4
Complete	262.5	34.1	50.0

It is evident that Eq. (7) is not properly calibrated to obtain the "weak/no structural damage" limit state described by EMS-98 for the structure under analysis. As a result of this, a noticeable difference between the RMA and the other fragility curves can be seen. According to this approach the D_1 spectral displacement for which the three-dimensional numerical model shows the first signs of damage would have, in fact, an extremely low probability of not being exceeded (3.3%). On the other hand the same spectral displacement is quite close to the HMA fragility curve median value (45.5% *vs.* the median value of 50%).

The same remarks can be made for the moderate limit state value compared to the FE analysis (CRA). D_2 has a probability of not being exceeded equal to 9.5% according to RMA and 60.8% according to HMA.

The discrepancies are obviously less marked for the two final limit states, e*xtensive* and c*omplete* for which there is less ambiguity in the definition of the limit state. The probabilities for the *extensive* damage state are 60.2% & 42.2% for HMA and RMA, respectively, *vs.* the median of 50%. As can be seen in Table **6**, the discrepancies reduce again for the *collapse* damage state which shows probabilities of 34.1% & 50% *vs.* the median of 50% for HMA and RMA, respectively.

Overall, comparison of the CRA limit states and HMA fragility curves in Fig. (**6**) indicate that the HAZUS fragility curves are reasonably accurate considering they have not been developed for single building types, but are applicable for a large population group of similar building types. This is particularly evident at the *slight, moderate* and *extensive* damage states. The *complete* limit state cannot be assessed since the numerical analysis fails at the reaching of *extensive* damage.

CONCLUSION

This paper has presented three different approaches to derive damage limits for a code designed reinforced concrete moment resisting frame structure. The methods investigated involved creating a detailed three-dimensional finite element model of the structure and applying lateral pushover forces according to Eurocode 8 to yield a capacity curve.

From this curve damage limits were obtained by:

- Visual observation of the crack patterns based on the HAZUS (1999) damage scale description (CRA);
- A mechanical approach based on the energy of the pushover curve and equivalent elasto-plastic SDOF curve (RMA).

Damage states were also obtained using the macro-seismic approach given in HAZUS (1999) under table form (HMA).

The damage states from RMA and HMA were used to build the fragility curves for *slight, moderate, extensive* and *complete* damage states and the values from CRA were assessed based on these fragility curves.

In general, the comparison of the HAZUS methodology (HMA) for fragility function derivation showed good agreement with the crack pattern given by the pushover analysis (CRA). The HMA results for the *slight*, *moderate* and *extensive* damage states showed good agreement, however showed poor agreement for the *extensive* damage state as this was not reached during pushover analysis. The HAZUS comparison should be taken in context that it is a statistical approach that was not developed for the specific building type under consideration. The Risk-UE methodology (RMA) showed very poor agreement for *slight* and *moderate* damage whilst reasonably poor agreement for *extensive* and *complete* damage states.

CONFLICT OF INTEREST

The authors confirm that this article content has no conflict of interest.

ACKNOWLEDGEMENTS

REFERENCES

[1]　M.A. Erberik, and A.S. Elnashai, "Seismic Vulnerability of Flat-slab Structures", In: *Mid-America Earthquake Center.* University of Il-linois at Urbana-Champaign: Urbana, 2003.

[2]　SHARE Consortium, *SHARE Seismic Hazard Harmonization for Europe - European Seismic Hazard Maps.* DGEB-Workshop, 27 May, 2014. Available from: http://www. share-eu.org/node/57

[3]　H. Crowley, "Introducing openquake, the interactive platform for collaborative earthquake risk assessment", In: *Proceedings of 10th National Conference on Earthquake Engineering*, Alaska, United States, 2014.

[4]　P. Gueguen, *Seismic Vulnerability of Structures.* Wiley: New York, United States, 2013.
[http://dx.doi.org/10.1002/9781118603925]

[5]　V. Silva, H. Crowley, H. Varum, R. Pinho, and R. Sousa, "Evaluation of analytical methodologies used to derive vulnerability functions", *Earthquake Eng. Struct. Dynam.,* vol. 43, no. 2, pp. 181-204, 2014.
[http://dx.doi.org/10.1002/eqe.2337]

[6]　P. Mouroux, E. Bertrand, M. Bour, B. Le Brun, S. Depinois, and P. Masure, "The european RISK-UE project: An advanced approach to earthquake risk scenarios", In: *Proceedings of the 13th World Conference on Earthquake Engineering*, Vancouver, Canada, 2004.

[7]　S. Lagomarsino, and S. Giovinazzi, "Macroseismic and mechanical models for the vulnerability and damage assessment of current buildings", *Bull. Earthquake Eng.,* vol. 4, no. 4, pp. 415-443, 2006.
[http://dx.doi.org/10.1007/s10518-006-9024-z]

[8]　HAZUS[®MH] MR4. *Multi-Hazard Loss Estimation Methodology: Earthquake Model.* Department of Homeland Security, FEMA: Washington, DC, 2003.

[9]　European Committee for Standardization, *Eurocode 8: Design of Structures for Earthquake Resistance" Part 1: General Rules, Seismic Actions and Rules for Buildings,* Terminology and General Criteria for Test Methods, 2004.

[10]　European Committee for Standardization, *European Committee for Standardization. CEN (2004b) Eurocode 2: Design of Concrete Structures – Part 1: General Rules and Rules for Buildings.* Product Requirements and Evaluation of Con-formity for Vehicle Restraint Systems, 2004.

[11]　*Simulia, Abaqus Finite Element Program Version 6.13,* Abaqus, 2013.

[12]　J. Lubliner, J. Oliver, S. Oller, and E. Onate, "A plastic-damage model for concrete", *Int. J. Solids Struct.,* vol. 25, no. 3, pp. 299-326, 1989.
[http://dx.doi.org/10.1016/0020-7683(89)90050-4]

[13]　*ABAQUS Analysis User's Manual.* ABAQUS, 2013.

[14]　E. Thorenfeldt, A. Tomaszewicz, and J. Jensen, "Mechanical properties of high-strength concrete and application in design", In: *Proceedings of the Symposium Utilization of High Strength Concrete*, Stavanger, 1987.

[15]　D.A. Hordijk, *"Local Approach to Fatigue of Concrete"*, Phd thesis, Delft University of Technology, 1991.

[16]　Comité Euro-Internationa du Béton, *CEB-FIP Model Code 2010, First Completed Draft,* Comité Euro-International Du Béton, Lausanne: Lausanne, Switzerland, 2010.

[17]　J. Lee, and G.L. Fenves, "Plastic-damage model for cyclic loading of concrete structures", *J. Eng. Mech.,* vol. 124, no. 8, pp. 892-900, 1998.
[http://dx.doi.org/10.1061/(ASCE)0733-9399(1998)124:8(892)]

[18]　T. Yu, J. Teng, Y. Wong, and S. Dong, "Finite element modeling of confined concrete-II: Plastic-damage model", *Eng. Struct.,* vol. 32, no. 3, pp. 680-691, 2010.
[http://dx.doi.org/10.1016/j.engstruct.2009.11.013]

[19]　R. Malm, *"Predicting Shear Type Crack Initiation and Growth in Concrete with Non-Linear Finite Element Method"*, Doctoral thesis, KTH, Department of Civil and Architectural Engineering, 2009.

[20]　European Seismological Commission, *European Macroseismic Scale 1998.* Joseph Beffort, Helfent-Bertrange: Luxembourg, 1998.